IL NUOVO CIMENTO **44 C** (2021) 20
DOI 10.1393/ncc/i2021-21020-y

COMMUNICATIONS: SIF Congress 2020

Neutronographic investigation of water transfer in porous limestones

G. PALADINI(*)

Dipartimento di Scienze Matematiche e Informatiche, Scienze Fisiche e Scienze della Terra, Università degli Studi di Messina - Messina, Italy

received 26 January 2021

Summary. — In this work, a comparative neutron radiography (NR) investigation was carried out on two different limestones, *i.e.*, *Pietra di Lecce* and *Pietra d'Aspra*, widely employed as building materials during the Italian baroque epoch (XVI–XVII century). The effect of the application of two different mm-thick layer of consolidating products, namely nanosilica (Nano Estel®) and nanolime (CaLoSiL®), was evaluated with the aim to qualitatively determine the best protective effectiveness against artificial external stimuli. In this framework, NR represents a well-established approach capable to highlight, in a completely non-destructive way, the water suction process by spontaneous imbibition occurring inside porous building materials. Water dynamics represents a powerful marker both for the evaluation of the extent of the weathering process and for the quantification of the consolidating action of a specific product. In our case, the water flow through the porous network of investigated limestones indicated two types of porosity, as revealed by the different "smoothness" of the corresponding water content *vs.* sample height profiles. The effect of the application of commercially available consolidants was distinguished by monitoring the wetting front positions as a function of time. The obtained results give insight into the different coating/limestone interaction mechanisms, whose understanding appears particularly useful for the selection of a proper intervention plan to be applied.

1. – Introduction

Consolidation is a general term which includes all processes aimed at retrieving the original structural properties of a stone after exposition to natural weathering phenomena, *i.e.*, salt crystallization, air pollution, biological attack and temperature jumps [1-4]. In this sense, a preliminary monitoring phase and an adequate petro-physical characterization of the investigated material represent fundamental pre-requisites for the correct choice of the intervention plan [5,6]. High efficiency and minimum aesthetical impact are

(*) E-mail: gpaladini@unime.it

usually preferred conditions in all those cases in which structures of interest in the field of cultural heritage (CH) are present. Nowadays, the use of nanosized consolidating and hydrophobic products in the treatment of building materials of historical monuments, capable to strongly reduce the impact of natural weathering, is of paramount importance in the field of conservation science. Added products must obey to standardized conditions which include: suitable penetration depth, uniform distribution within the porous network of the stone and minimum appearance alterations. All these features are deeply related to the porosity of the stone, which is the reason why it is considered one of the most significant parameters for conservation purposes. The application of such coatings can be usually optimized starting from the knowledge of the distribution of the consolidant nanoparticles onto the stone surface. Moreover, variations in the physical properties of the stone after consolidation, in terms of susceptibility to weathering, should also be taken into account. Among the possible natural weathering phenomena which may affect the integrity of construction materials, penetration of water inside the porous structure represents the main cause of deterioration, leading to the formation of alveolar structures and/or encrustations. Water transfer through spontaneous imbibition is related to the degree of accessible porosity and deeply regulates the material consumption over time.

Fluid transport can be properly visualized by NR. In fact, as well known, low- and high-hydrogen content materials can be properly distinguished, being characterized by different neutron attenuation coefficients (NACs). High NAC values are achieved in boron, gadolinium, hydrogen, cadmium, etc. On the contrary, common elements characterizing natural stones (*i.e.*, limestones), such as aluminum, calcium and silicon, have lower NACs with respect to the aforementioned elements. Such discrepancy represents the first source of contrast in neutron-based radiographs. In this sense, neutron radiography represents a powerful approach for the evaluation of the height of the wetting front as well as its 3D distribution, since all hydrogen-rich fluids hold higher neutron attenuation coefficients with respect to elements of which limestone specimens are typically made up. Neutron radiography has already been applied to map the 3D water content distribution for a wide range of porous construction materials [7-10]. In particular, movement and 3D distribution of water within the porous network of bricks [11], rocks [12] and concretes [13] have been successfully evaluated. The degree of internal homogeneity plays a foundamental role in determining the profile of the height of the water front ($y(t)$) as a function of time. In particular, according to the Lucas-Washburn (L-W) equation, a linear trend of $y(t)$ *vs.* $\sqrt{t}$ in structures having a mono-dimensional and uniformly distributed porosity should be expected (diffusion-like process). However, discrepancy from the aforementioned behaviour can be often achieved, due to an intrinsically disordered porous distribution. In addition, violations from the natural diffusion uptake at the beginning or after a prolonged contact time ("anomalous diffusion") can also provide useful indication about the occurring of specific stone/consolidants interactions.

In the light of the aforementioned considerations, the aim of this work was the evaluation, through a completely non-invasive approach, of the effect that the pore structure and the consolidant/stone interactions exert on the water transport behaviour exhibited by two investigated limestones, *i.e.*, *Pietra di Lecce* (LS) and *Pietra d'Aspra* (AS). The susceptibility to weathering of both stones before and after consolidation with two commercially available protective coatings, *i.e.*, nanosilica (nano-SiO_2, NNS) and nanolime ($Ca(OH)_2$, NNL) was accomplished with the aim to highlight the consolidating efficiency of the two used products. In particular, samples were exposed to different accelerated weathering tests (salt crystallization and temperature/relative humidity jumps (T/RH)) in order to assess their susceptibility. After each treatment, the water flow and 3D

distribution were monitored as a function of time. The obtained results could provide useful insight in the field of conservation science as they can be used to design optimized procedures for the maintenance of buildings/objects and for the preservation of their artistic and aesthetic value.

2. – Materials and methods

2˙1. *Materials.* – *Pietra di Lecce* (LS) and *Pietra d'Aspra* (AS) are two calcite-based bio-calcarenites extensively employed as building materials around the Salento (Puglia, southern Italy) and Palermo (Sicily, southern Italy) areas, respectively. More in detail, LS can be regarded as a wackestone of a typical light-yellow colour made up of micritic fractions of clay minerals mixed with other minor insoluble residues (clay minerals). The total open porosity, distributed homogeneously throughout the crystalline network, is around 40%, with a pore radius ranging from 0.5 μm to 4 μm [14,15]. On the contrary, AS can be regarded as a grainstone [14] characterized by a non-uniform/heterogeneous internal grain size distribution. Previous analysis through thin-section microphotographs [16] highlighted a two-fold distribution of modes associated to calcareous bioclasts and lithic fragments, respectively. In this sense, it is possible to distinguish AS lithotypes according to the dimension of grains in *medium-to-fine* arenites (0.5–0.125 mm) and *coarse-to-medium* arenites (2–0.5 mm) [17]. Furthermore, poorly connected pores having a wide range of dimensions and shapes can be recognized, providing values of open porosity accessible for water which strongly depend on the used variety. It is worth underlying that both stones are strongly affected by several deterioration phenomena including alveolization, biological attacks, salt crystallization and erosion. In this sense, water imbibition through capillary suction represents the key factor to study all the aforementioned decay processes.

2˙2. *Neutron radiography.* – Time-lapsed neutron radiographs of 14 different samples were collected through the cold neutron imaging station IMAGINE of the Laboratoire Léon Brillouin (LLB) at the Orphée Reactor, in Saclay (F) (see fig. 1). The acquisition of neutron radiographs of non-consolidated and artificially weathered LS and AS samples ($\sim 5 \times 5 \times 2\,\mathrm{cm}^3$) was first assessed. After that, both samples were brushed with two commercially available consolidants, *i.e.*, Nano Estel® (CTS srl, Vicenza, Italy) and CaLoSiL® (Bresciani srl, Milano, Italy), until saturation. After 28 days of curing time, artificial weathering tests (15 cycles of salt crystallization and temperature/relative humidity (T/RH) jumps after three cycles of salt crystallization) were carried out on both treated and untreated samples following the procedure described in ref. [18] (see table I for details).

A spatial resolutions of ~ 250 μm was provided by increasing the L/D ratio up to 400, with L equal to the distance between the neutron beam entrance aperture and the image plane (400 cm) and D the diameter of the collimator aperture (1 cm). In this way, high absorption contrast values (with a resolution of 0.1%) were also achieved. The initial flux of neutrons provided by the Orphée Reactor was of $\sim 2 \times 10^7$ n cm^{-2} s^{-1}. Dynamic radiographs have been produced by measuring how much of the impinging radiation, passing through the sample, is attenuated or transmitted. In this sense, neutrons allow to easily record the distribution of water and its evolution in limestone materials (key elements: Ca, C, O, etc.) with extremely high contrasts, due to the high sensitivity of neutrons to hydrogens. In our case, transmitted neutrons were detected by means of a sCMOS ANDOR NEO camera coupled to a Canon EFS 60 mm F/2.8 Macro USM.

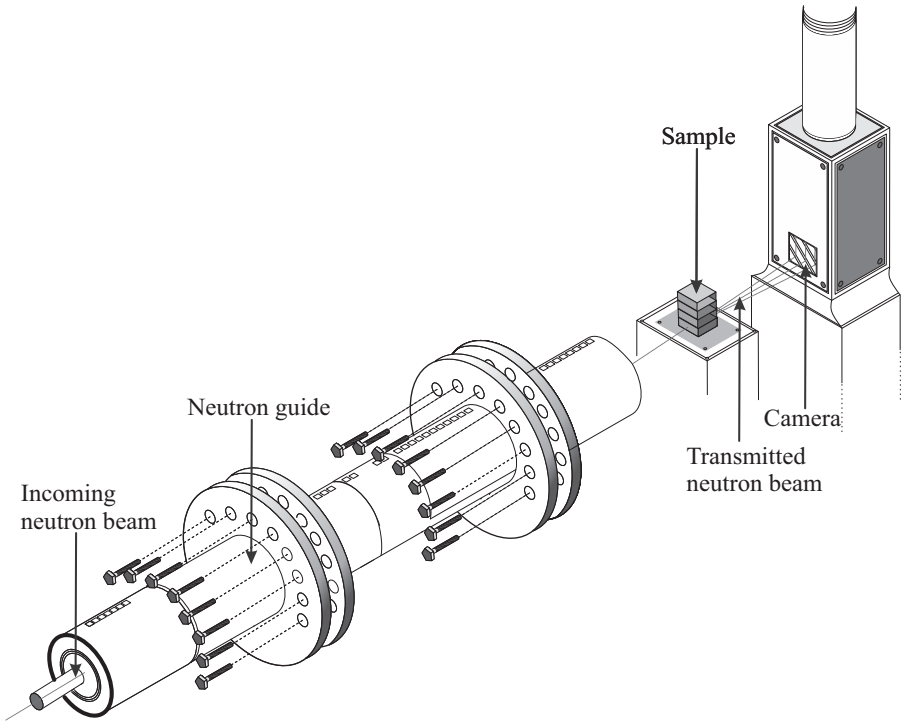

Fig. 1. – Schematic representation of the neutron imaging spectrometer IMAGINE.

The experimental strategy consisted in placing the investigated specimens one by one within an aluminum holder onto a 10 mm thickness filter paper pack (Kaltek S.r.l., Padova, Italy), which allows the acquisition of radiographs of the entire sample volume. The water absorption dynamics was recorded by collecting neutron images in a sequential mode starting from the manual introduction of water into the aluminum container, until full saturation of the specimen. In the case of LS stones, an exposition time of 10 s was used for all the investigated samples. The only exception was made for LS1, for which an

TABLE I. – *List of specimens under investigation together with a description of the used products and accelerated weathering tests applied. LSTQ and ASTQ were used as references for comparisons.*

Sample	Consolidant	Artificial weathering test
LS1 (AS1)	Nano Estel®	climatic chamber (T/RH)
LS2 (AS2)	Nano Estel®	salt weathering (15 cycles)
LS3 (AS3)	Nano Estel®	not weathered
LS4 (AS4)	CaLoSiL®	climatic chamber (T/RH)
LS5 (AS5)	CaLoSiL®	salt weathering (15 cycles)
LS6 (AS6)	CaLoSiL®	not weathered
LSTQ (ASTQ)	untreated	Not weathered

exposition time of 40 s was needed. In AS, neutron radiographs were collected with an exposure time of 40 s, except for AS4, for which an exposition time of 10 s was employed. It is worth noting, however, that in any case measurements were acquired for no longer than $\sim$ 20 h, even though a full water saturation condition was not completely reached.

A detailed description of the raw images pre- and post-processing strategy adopted is presented in detail elsewhere [16, 19]. The water content was quantified following the procedure described by Kim *et al.* [20]. Quantitative information was evaluated following calibration of the acquired transmission values. For this purpose, a staircase-like holder having 12 known values of water contents, characterized by standardized thickness, was used to properly evaluate the value of the water attenuation coefficient. The latter parameter was then used to correctly calculate the percentage of absorbed water contained within the structure of the investigated limestones.

3. – Results and discussion

Selected neutron radiographs collected for sample LS1 and AS1 at three different time-steps after water exposure are displayed in fig. 2, as an example.

The water suction dynamics exhibited by LS1 and AS1 specimens appear completely different from each other (see fig. 2). Such variations are also revealed for all the re-

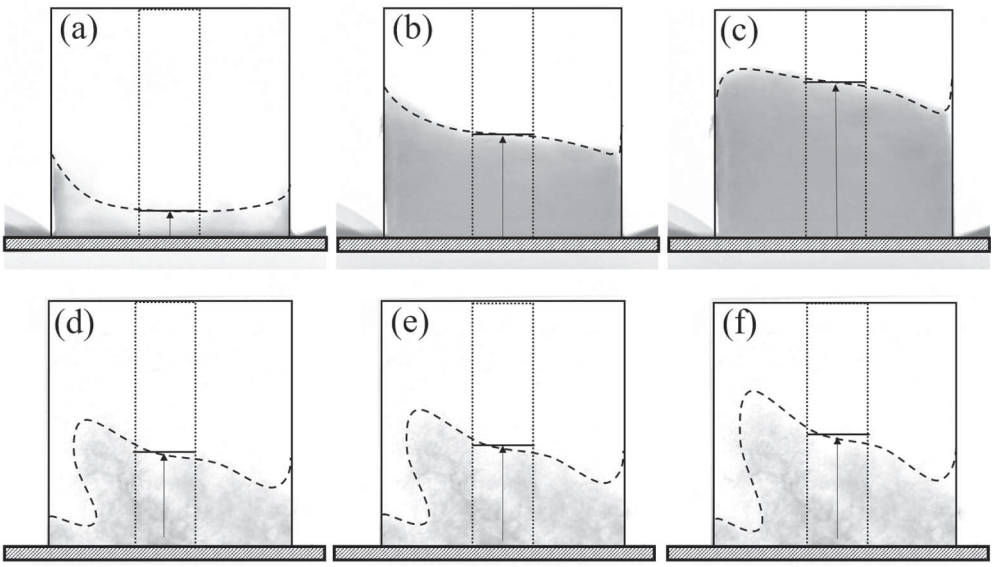

Fig. 2. – Grey-scaled neutron images of the time-dependent water imbibition process occurring in LS1 ((a)–(c)) and AS1 ((d)–(f)) after 40 s ((a), (d)), 2000 s ((b), (e)) and 3960 s ((c), (f)) of water contact. As can be clearly observed, the presence of water within the stone porous network is evidenced by the presence of a water-poor and water-rich phase within the investigated sample volume (white and dark grey regions). Dashed lines in each panel indicate the distribution of water during the suction toward the top of the specimen. In our case, the quantitative evaluation of the water content is accomplished starting from the selection of a *region-of-interest* (ROI) contained within the 5×5 cm^2 frontal section of each image (displayed in the figure as dotted boxes). Then, positions of the water front (horizontal line within each ROI) as a function of time can be properly quantified and monitored. Finally, hatched areas at the bottom of each panel account for the initial manually added water thickness.

maining LS and AS samples (data not shown), evidencing the strong influence of the stone internal structure on the resulting water suction behaviour. The wetting region becomes visible for almost all the investigated samples already at the first stage of the absorption test (40 s), although their evolution appears quite different. In the case of LS1, the onset of a well-defined boundary between the water-poor and water-rich zone, in conjunction with a regular rise of the wetting front, can be clearly observed. Both aspects fully support the existence of a uniform micro-texture characterized by a high inter-pore connection degree [14, 15]. Conversely, in the case of AS1, an irregular water flow due to a non-uniform size of the individual natural components and/or pores can be recognized, leading to visible distortions of the path with respect to that observed in LS1 sample (see, for example, fig. 2(b), (e)). Such alterations can be reasonably ascribed to the development of a preferential pathway for the liquid water during natural imbibition.

The susceptibility to weathering in treated and untreated LS and AS samples was quantitatively evaluated starting from the analysis of typical plots of water content as a function of the sample height (fig. 3). From a first inspection of fig. 3 we can state that, regardless of whether the stone has been consolidated/artificially aged or not, the amount of absorbed water in LS samples is found to be always greater than that in AS ones. In particular, the wt% values observed for LS1, LS2, LS3, LS4, LS5, LS6 and LSTQ are $\sim$ 4% ($\sim$ 0.8% in AS1), $\sim$ 2.5% ($\sim$ 0.9% in AS2), $\sim$ 3.6% ($\sim$ 3% in AS3), $\sim$ 4.2% ($\sim$ 3% in AS4), $\sim$ 3.5% ($\sim$ 3.2% in AS5), $\sim$ 5.2% ($\sim$ 2.9% in AS6) and $\sim$ 5% ($\sim$ 2.5% in ASTQ), respectively. This evidence can be ascribed to dissimilarities in the inner structural features (between *Pietra di Lecce* and *Pietra d'Aspra*) as well as to the different porosimetry. In fact, as well known from the classical theory of transport phenomena in porous media, the shape and dimension of pores play a foundamental role in determining the driving force acting on the liquid water. In particular, according to the Young-Laplace equation [21], larger air "bubbles", as those present in treated and untreated AS samples, require more time to be filled than smaller ones. Accordingly, after $\sim$ 30 min of exposure, the aforementioned wt% discrepancy can be reasonably associated to a remarkable difference in the number of cavities filled with water, higher in LS samples (smaller pores) than in AS ones (larger pores). A further explanation can be derived by taking into account the degree of pores inter-connection. A poorly connected porous capillary network provides a hindered path for the liquid water. Hence, during the first $\sim$ 30 min of the absorption test, a diminished water amount in AS samples with respect to LS ones was expected, being the degree of pores connection as well as the transfer kinetics much higher and regular in LS than in AS. The aforementioned aspects also characterize the different "smoothness" of the observed water content profiles displayed in fig. 3. In fact, whereas in all treated and untreated LS limestones extremely regular plots can be recognized, the same is not true for AS specimens, for which visible indented evolutions occur. The latter reasonably reflect the presence of hardly/easily accessible localized regions (of the order of mm) across which the liquid transport takes place. Such features can be due to the well-known bimodal distribution of AS principal/secondary constituents, leading to a non-uniform 3D water distribution over the scanned sample height, regardless of the type of treatment or artificial weathering applied.

Let us focus the attention on the effect that the application of NNS/NNL consolidants, and artificial weathering tests, exerts on the water transport behaviour of both investigated limestones. First of all, in the case of LS specimens, values of the height reached by the water front (see fig. 3) in consolidated samples (whether they are artificially aged (AL1, AL2, AL4, AL5) or not (AL3 and AL6)) turned out to be always lower than, or comparable to, the one observed for LSTQ (reference). Same considerations can be made

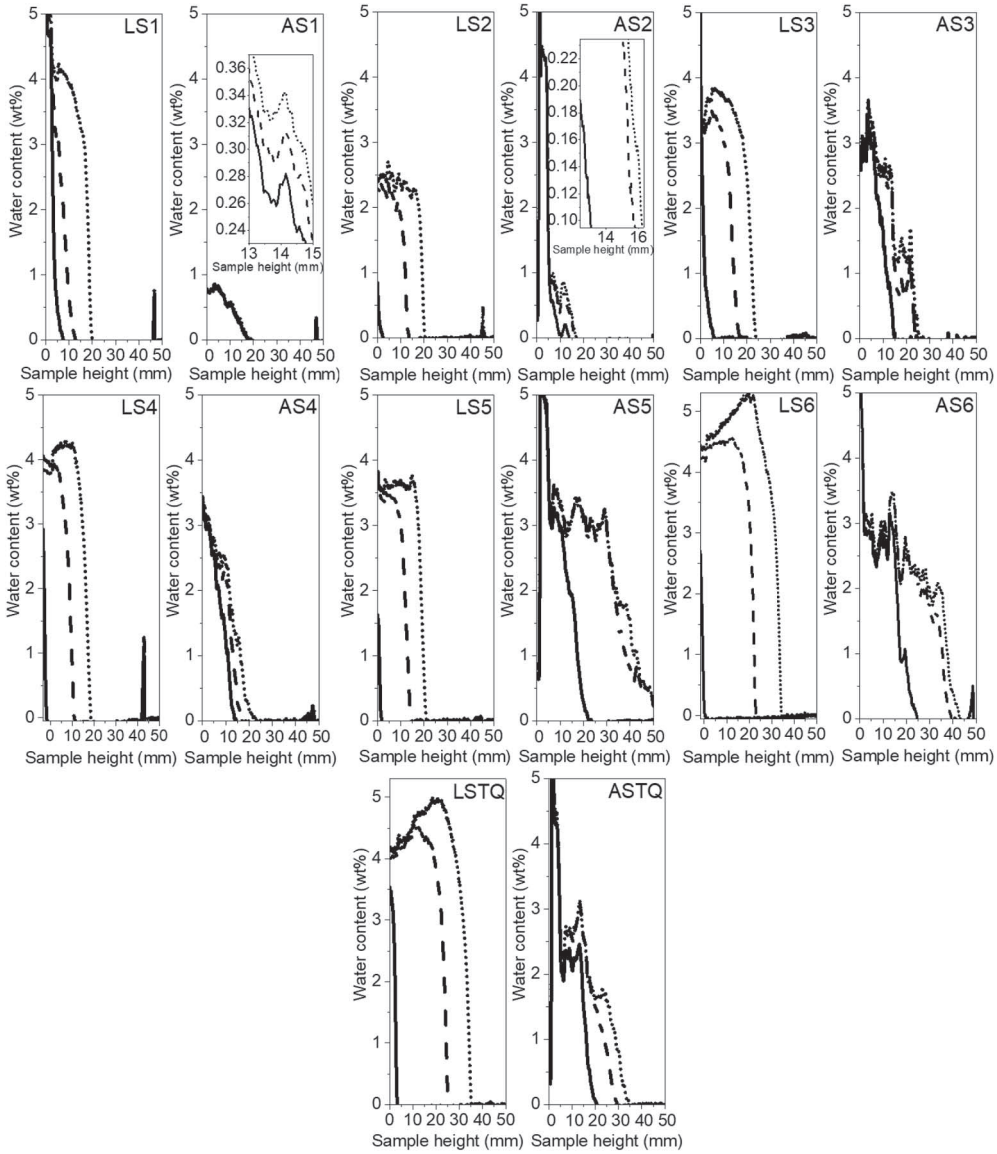

Fig. 3. – Water content profiles (expressed in wt%) as a function of the sample height calculated following the analytical strategy described in refs. [16, 19]. In order to compare the water absorption behaviour exhibited by both investigated stones, plots reported in this figure have been collected for no longer than $\sim$ 30 min after the water exposure. In particular, continuous, dashed and dotted lines in each panel account for the water content profile calculated for the first neutron-radiograph acquisition (see sect. **2**˙2 for details), after $\sim$ 15 min and after $\sim$ 30 min, respectively. Only in the case of AS1 and AS2, the two insets display different detailed regions of the wt% *vs.* sample height plane.

for AS specimens, providing an experimental evidence of the consolidation ability of both NNS and NNL products on the investigated stones. However, results reported in fig. 3 indicate remarkable differences in the consolidating action according to the used product. In particular, the observed values of water content and height of water front in NNS-

treated specimens not subjected to any artificial weathering test (LS3 and AS3) were found to be lower with respect to NNL-treated ones (LS6 and AS6). Moreover, by comparing the aforementioned values with the corresponding reference materials (LSTQ and ASTQ), no differences are evidenced for NNL-treated limestones, LS6 and AS6, whose wt% and height of water front appear almost similar to those in LSTQ and ASTQ. On the contrary, a diminishing of the height of the wetting front down to $\sim$ 21 mm and $\sim$ 20 mm in LS3 and AS3 ($\sim$ 34 mm and $\sim$ 31 mm in LSTQ and ASTQ, respectively), was highlighted. Being the water transport in porous rocks the main factor affecting the durability, according to the aforementioned considerations, we can state that the presence of a mm-thick layer of NNS positively affects the susceptibility to weathering of both investigated stone more than NNL at the early stage of the absorption test. NNS acts as capping agent with respect to the open pore network accessible for water, showing a super-hydrophobic behaviour. Occlusion of pores leads to the obstruction of some initially available liquid routes within the stone structure, causing a hindering in the water capillary suction kinetics. It is worth noting that such condition is generally highly demanded in conservation science since it favours the preservation of the natural stone characteristics by reducing the risk of decohesion, erosion and of inclusion of unwanted substances coming from the surrounding environment.

The latter mechanism is, instead, not revealed in LS6 (NNL-treated) which behaves like the reference one (LSTQ) in terms of water absorption (the water reaches approximatively $\sim$ 34 mm and $\sim$ 31 mm, respectively). Interestingly, for what concerns AS6, the application of NNL consolidant seems to slightly favour the water rise through capillarity within the porous network, as suggested by the value reached by the water front ($\sim$ 40 mm) after $\sim$ 30 min of suction. The behaviour exhibited by LS6 and AS6 specimens, as opposed to what has been observed for LS3 and AS3, indicates that the NNL-consolidant/stone interactions allow the pore network to host water molecules with a greater effectiveness than NNS-treated samples (LS3 and AS3), or reference materials (LSTQ and ASTQ). This is a direct consequence of a retained open porosity which allows the network of both stones to maintain a certain "mobility", since the pores are not totally obstructed. The latter condition acts as "damping" agent against the naturally occurring high crystallization pressures, responsible for the development of small fractures and distortions within the investigated stones. In this sense, NNL product also enhances the durability of both *Pietra di Lecce* and *Pietra d'Aspra* stone although the application of NNS, thanks to the total obstruction of the outer pore layer extending over the NNS-impregnated thickness, seems to be the most efficient one.

As far as the effect of artificial weathering on both LS and AS stones is concerned, the analysis of the water absorption behaviour exhibited by samples exposed to thermal and RH treatments (in a climatic chamber), namely LS1, AS1, LS4 and AS4, and 15 cycles of salt crystallization, namely LS2, AS2, LS5 and AS5, was finally carried out. Concerning samples exposed to T/RH jumps after three cycles of salt crystallization, the applied artificial treatment causes major variations in the water suction kinetics in AS specimens (AS1 and AS4) rather than LS ones (LS1 and LS4) at the early stage of the absorption test. In particular, the wt% values in AS1 and AS4 turned out to be equal to $\sim$ 0.8% and $\sim$ 3%, respectively. It is worth noting that, according to previous experimental results on similar systems [22], thermal/RH stresses usually modify both pores connection degree and 3D distribution due to transitions occurring between the thenardite and mirabilite phases. Such process leads to the enlargement of initial micro-fractures within the porous stone network, responsible for the observed water suction kinetics alterations (if compared to both the corresponding only treated (not weathered) AS3 and AS6

samples and reference ASTQ one). However, the almost total obstruction of accessible pores provided by the NNS product strongly reduces the wettability of the AS1 material ($\sim$ 0.7% and $\sim$ 15 mm), positively affecting its susceptibility against artificial T/RH microclimatic stresses. Finally, in the case of LS1 and LS4, the application of both consolidants does not seem to affect the water absorption to the same extent as that observed for AS1 and AS4 against T/RH jumps. In fact, an almost similar transport behaviour with non-weathered LS3 and LS6 samples can be observed, except for a slight reduction of the mean penetration depth reached by water.

Concerning samples subjected to 15 cycles of salt crystallization, NNS-treated limestones (LS2 and AS2) show a reduced water content and height of the water front values with respect to samples brushed with NNL (LS5 and AS5). In AS2, the amount of absorbed water was found to be equal to $\sim$ 0.9% (reaching approximatively $\sim$ 18–20 mm), supporting the assertion that NNS provides a better consolidation efficacy with respect to NNL at the early stage of the absorption test. In fact, the wt% values in AS5 turned out to be always higher with respect to both AS2 and ASTQ samples. This occurrence, also applicable in LS, can be explained by considering that salt crystallization cycles may provide new "routes" within the porous network of the stone due to the formation of stress-induced cracks and fractures. Such new channels should be considered as preferential pathways for the liquid solution, which now penetrates the structure more efficiently.

All the reported NR results suggest that the application of nanosilica (Nano Estel®) on both investigated limestones, subjected to different artificial weathering tests, hinders the water transfer better than nanolime (CaLoSiL®) at the early stage of the water absorption test. However, the different penetration depth of the consolidating products should be also taken into account for the analysis of the water suction process in porous structures. In fact, a more or less extensive penetration of the coating is likely to change the dynamics of the imbibition process, causing slight deviations/alterations in the water 3D distribution and kinetics observed by NR.

4. – Conclusions

Neutron radiography was here employed on two different types of limestones, *i.e.*, *Pietra di Lecce* and *Pietra d'Aspra*, in order to comparatively evaluate the susceptibility to weathering starting from the analysis of the water absorption behaviour. For this purpose, the effectiveness of two different commercially available products (nanosilica (Nano Estel®) and nanolime (CaLoSiL®)), acting as consolidating agents against artificial weathering phenomena, was successfully investigated. The water motion inside the porous network of both stones allowed us to highlight, in a non-destructive way, the close relationship between the inner porous distribution and the resulting liquid kinetics. Trends of water content as a function of the sample height, maximum amounts of absorbed water and wetting front positions obtained point out a better performance of nanosilica with respect to nanolime. Finally, a description of the effect that artificial weathering exerts on the inner structure of both LS and AS samples was addressed. It is worth noting that the high resolution achieved through NR allows the quantification of localized water quantities within the calcite-based calcarenites thanks to the water/stone neutron cross-section differences. In this sense, indirect information about inner stone alterations (formation of fracture, phase transitions, etc.) was also obtained.

* * *

The author acknowledges his supervisors D. Majolino, V. Crupi and V. Venuti (University of Messina) and his colleagues M. F. La Russa, L. Randazzo, N. Rovella, M. Ricca (University of Calabria) and G. Montana (University of Palermo) for their precious contribution and useful discussions to the research topic presented in this work. Finally, the author would like to thank the Laboratoire Léon Brillouin (LLB), CEA Saclay (France), for the beamtime and in particular F. Ott as local contact.

REFERENCES

[1] Bottari C., Crisci G. M., Crupi V., Ignazzitto V., La Russa M. F., Majolino D., Ricca M., Rossi B., Ruffolo S. A., Teixeira J. and Venuti V., *Appl. Phys. A*, **122** (2016) 721.
[2] Hammecker C., *Pure Appl. Geophys.*, **145** (1995) 337.
[3] Mohammad B. K., *Electron. J. Geotech. Eng.*, **8** (2003) 1.
[4] Leith S. D., Reddy M. M., Ramirez W. F. and Heymans M. J., *Environ. Sci. Technol.*, **30** (1996) 2202.
[5] Calia A., Laurenzi Tabasso M., Mecchi A. M. and Quarta G., *Geol. Soc. Spec. Publ.*, **391** (2013) 139.
[6] La Russa M. F., Belfiore C. M., Fichera G. V., Maniscalco R., Calabró C., Ruffolo S. A. and Pezzino A., *Constr. Build. Mater.*, **77** (2015) 7.
[7] Pel L., Ketelaars A. A. J., Adan O. C. G. and van Well A. A., *Int. J. Heat Mass Transfer.*, **36** (1993) 1261.
[8] Masschaele B., Dierick M., Cnudde V., Van Hoorebeke L., Delputte S., Gildemeister A., Gaehler R. and Hillenbach A., *Radiat. Phys. Chem.*, **71** (2004) 807.
[9] Abd A. E.-G. E., Czachor A., Milczarek J. J. and Pogorzelski J., *IEEE Trans. Nucl. Sci.*, **52** (2005) 299.
[10] Hassanein R., Meyer H. O., Carminati A., Estermann M., Lehmann E. and Vontobel P., *J. Phys. D: Appl. Phys.*, **39** (2006) 4284.
[11] Zhou X., Desmarais G., Vontobel P., Carmeliet J. and Derome D., *J. Build. Phys.*, **44** (2020) 251.
[12] Winkler B., Kahle A. and Hennion B., *Phys. B Condens. Matter*, **385–386** (2006) 933.
[13] Hanžič L., Kosec L. and Anžel I., *Cem. Concr. Compos.*, **32** (2010) 84.
[14] Dunham R. J., *Classification of carbonate rocks according to depositional texture*, in *Classification of Carbonate Rocks: A Symposium*, edited by Ham W. E. (American Association of Petroleum Geologists) 1962, pp. 108–121.
[15] Zezza F., *Rass. Tec. Pugl.*, **3-4** (1974) 3.
[16] Randazzo L., Paladini G., Venuti V., Crupi V., Ott F., Montana G., Ricca M., Rovella N., La Russa M. F. and Majolino D., *Appl. Sci.*, **10** (2020) 6745.
[17] La Duca R., *Boll. Ord. Ing. Palermo*, **3–4** (1967) 7.
[18] Benavente D., García Del Cura M. A., Bernabéu A. and Ordóñez S., *Eng. Geol.*, **59** (2001) 313.
[19] Randazzo L., Venuti V., Paladini G., Crupi V., Majolino D., Ott F., Ricca M., Rovella N. and La Russa M. F., *J. Cult. Herit.*, **46** (2020) 31.
[20] Kim F. H., Penumadu D. and Hussey D. S., *J. Geotech. Geoenviron. Eng.*, **138** (2011) 147.
[21] Lucero C. L., Bentz D. P., Hussey D. S., Jacobson D. L. and Weiss W. J., *Phys. Procedia*, **69** (2015) 542.
[22] Steiger M. and Asmussen S., *Geochim. Cosmochim. Acta*, **72** (2008) 4291.